Stresses in semiconductors: *Ab initio* calculations on Si, Ge, and GaAs

O. H. Nielsen

Nordisk Institut for Teoretisk Atomfysik, Blegdamsvej 17, DK-2100 Copenhagen, Denmark*
and Xerox Palo Alto Research Center, 3333 Coyote Hill Road, Palo Alto, California 94304

Richard M. Martin

Xerox Palo Alto Research Center, 3333 Coyote Hill Road, Palo Alto, California 94304
(Received 4 March 1985)

Explicit formulas for the calculation of stress are presented based on the stress theorem and the local-density-functional approximation. Norm-conserving pseudopotentials are applied in a plane-wave basis for calculations on the semiconductors Si, Ge, and GaAs. Besides the lattice constants and bulk moduli, complete sets of elastic constants are given, together with the optical Γ phonon frequencies and internal-strain parameter ζ. Electronic charge density structure factors, deformation potentials, and strain-induced splittings of phonons are given, as well as the nonlinear third-order elastic constants. Good agreement with experiment is found throughout, except for persistent deviations from the x-ray diffraction values for ζ.

I. INTRODUCTION

Calculation of total energy is a fundamental method capable of describing ground-state properties of a wide range of solids. Much of the work in recent years relies on the local-density approximation[1,2] for exchange and correlation, where a single-particle Schrödinger equation is solved self-consistently. The nontrivial problem of evaluating the total energy to a precision of 10^{-5} or better has in recent years been the subject of many investigations using various techniques.[3–8] In particular, the pseudopotential technique has been utilized for calculations of lattice constants and phase transitions,[9] "frozen" phonons,[4,7,10] complete phonon-dispersion curves and other properties,[10,11] and elastic properties.[12] There are several reviews of recent work in this area.[13]

Notwithstanding the role of total energy as the fundamental quantity in density-functional theory and other theories of interacting many-body systems, the utility of its derivatives with respect to structural parameters has been clearly demonstrated in recent years. Firstly, the "Hellmann-Feynman" theorem[14] (which was originally derived by Ehrenfest[15]) gives the force conjugate to atomic position. The great simplifications arising from direct calculation of forces are evident, e.g., from recent applications to phonon properties where many inequivalent forces can be calculated from a single self-consistent calculation. Accurate results have been obtained using forces, despite the traditional experience that forces cannot be accurately calculated.[16] Applications cover, e.g., frozen phonons,[10] phonon dispersion,[11] internal degrees of freedom in complex crystals,[17] and surface reconstruction.[18,19]

Secondly, the stress tensor in a solid is the derivative of the total energy with respect to the strain tensor. Recently, we have derived the stress theorem[12] which gives analytic expressions for the stress tensor (preceding paper,[20] hereafter referred to as I). A similar expression was given

earlier by McLellan.[21] This result is a generalization of the virial theorem[22,23] for pressure, and offers together with the force theorem the complete description of the equation of state of any finite or infinite system. The detailed interpretation of stresses and forces and their interconnection is given in paper I.

The purpose of the present paper is to investigate a number of properties of perfect crystalline solids, which are particularly convenient to study via evaluation of the macroscopic stress tensor together with forces and total energy. The results could in principle be obtained through extensive calculations of the total energy versus distortion parameters with subsequent fitting and differentiation. However, dramatic gains in efficiency are achieved with the present method which enables calculations that would otherwise be intractable.

The most straightforward application is the determination of equilibrium lattice parameters. In the present study cubic crystals of a fixed symmetry are considered, and the problem simplifies to the vanishing of the isotropic pressure versus lattice constant.[12] This problem is found to be significantly easier than locating the minimum of the total-energy curve. In more general crystals neither the unit-cell shape and dimension nor the atomic positions are given by symmetry, and the optimization problem involves multidimensional parameters such as c/a ratios and interatomic distances. In such cases stress and force become even more powerful tools, as shown by the recent work[17,24] on low-symmetry crystal structures using the methods derived here.

The evaluation of the elastic properties of solids is greatly simplified by direct calculations of stress, in the same way that direct evaluation of restoring forces due to atomic displacements leads to simplifications.[10,11] For an arbitrary strain in the solid, all components of the stress tensor may be computed from a single calculation. For example, harmonic elastic constants are for small strains defined as the ratio of stress to strain. It is furthermore

possible to go to large strains where the stresses are very anharmonic. A related structural property of solids is the possibility of internal degrees of freedom appearing in the unit cell when its symmetry is lowered sufficiently by the strain. An example is the diamond lattice strained along the [111] axis, where the [111] bond length is no longer related to the three other atomic bonds. Simultaneous calculations of stress and force enable an efficient solution of this problem, as demonstrated in Ref. 12 and in the present paper.

We explore in this paper the calculation of the lattice constants and a number of properties related to low-symmetry distortions of crystals, exemplified by the semiconductors Si, Ge, and GaAs, using the *ab initio* pseudopotential technique.[25−27] The present calculations include all three cubic elastic constants c_{11}, c_{12}, and c_{44}, and constitute the first complete sets calculated for any material with an *ab initio* method. The paper contains in Sec. II a formulation of the stress theorem suited for calculations with plane-wave basis sets, and in Sec. III a description of the method for *ab initio* pseudopotential calculations. Section IV describes the equilibrium structure and charge density. Section V addresses the harmonic elastic properties. Another effect of the application of uniaxial strain is the splitting of states that are degenerate in the cubic crys-

tal. In some cases the splittings can be observed by optical experiments, as will be considered in Sec. VI for deformation potentials, and in Sec. VII for phonon splittings. The nonlinear elastic properties of Si under large strains is the topic of Sec. VIII.

II. RECIPROCAL-SPACE EXPRESSION FOR STRESS

The local-density-approximation (LDA) expression for total energy[1] consists of the single-particle energies (kinetic plus potential energy, or alternatively the sum of eigenvalues) of the occupied states, Hartree electron repulsion, the exchange and correlation energy, and the ion-ion Madelung energy. For some calculational schemes, such as the pseudopotential method employed in the present work, it is advantageous to express all quantities in reciprocal space where a manageable plane-wave basis set gives a high calculational accuracy. This method was described by Wendel and Martin[4] and explicit reciprocal-space expressions were given by Ihm, Zunger, and Cohen[28] who also covered nonlocal potentials and Hellmann-Feynman forces. The expressions were elaborated by Yin and Cohen.[29]

The expression for the total energy E_{tot} (in atomic Hartree units) per unit-cell volume Ω is[28]

$$E_{\text{tot}}/\Omega = \sum_{\mathbf{k},\mathbf{G},i} |\Psi_i(\mathbf{k}+\mathbf{G})|^2 \frac{\hbar^2}{2m}(\mathbf{k}+\mathbf{G})^2 + \frac{1}{2}4\pi e^2 \sum_{\mathbf{G}}' \frac{|\rho(\mathbf{G})|^2}{G^2} + \sum_{\mathbf{G}} \epsilon_{\text{xc}}(\mathbf{G})\rho^*(\mathbf{G}) + \sum_{\mathbf{G},\tau}' S_\tau(\mathbf{G})V_\tau^L(G)\rho^*(\mathbf{G})$$

$$+ \sum_{\mathbf{k},\mathbf{G},\mathbf{G}',i,l,\tau} S_\tau(\mathbf{G}-\mathbf{G}')\Delta V_{l,\tau}^{\text{NL}}(\mathbf{k}+\mathbf{G},\mathbf{k}+\mathbf{G}')\Psi_i(\mathbf{k}+\mathbf{G})\Psi_i^*(\mathbf{k}+\mathbf{G}') + \left[\sum_\tau \alpha_\tau\right]\left[\Omega^{-1}\sum_\tau Z_\tau\right] + \Omega^{-1}\gamma_{\text{Ewald}}, \qquad (1)$$

where $\mathbf{k}$ extends over the first Brillouin zone, $\mathbf{G}$ are the reciprocal-lattice vectors, Ψ is the wave function, i denotes the occupied states for a given $\mathbf{k}$, ρ is the charge density, $\sum'$ denotes a sum excluding $\mathbf{G}=0$, τ labels the atoms in the unit cell, $S_\tau(\mathbf{G})$ is the structure factor, V^L is a local (l-independent) spherically symmetric potential, l labels the angular momentum ($l=0,1,2,\ldots$), ΔV^{NL} is a nonlocal (l-dependent) correction superposed on V^L, α_τ denotes the average non-Coulomb part of V^L,[28] Z_τ is the ionic charge, and γ_{Ewald} the Madelung energy of point ions in a constant neutralizing background.[30] Equation (1) may be rewritten by noting that kinetic plus potential energy equals the sum of eigenvalues, yielding an equivalent expression for total energy.[28]

The average stress $\sigma_{\alpha\beta}$ is derived from Eq. (1) by applying the scaling procedure of Ref. 20, $\mathbf{r}\rightarrow(1+\epsilon)\mathbf{r}$. A symmetric strain tensor $\epsilon_{\alpha\beta}$ transforms, to first order, $\mathbf{G}$ into $(1-\epsilon)\mathbf{G}$. Since $\Omega\rho(\mathbf{G})$ and $S_\tau(\mathbf{G})$ are invariant under scaling, we find the average stress:

$$\sigma_{\alpha\beta} = \Omega^{-1}\frac{\partial E_{\text{tot}}}{\partial \epsilon_{\alpha\beta}} = \frac{\hbar^2}{m}\sum_{\mathbf{k},\mathbf{G},i} |\Psi_i(\mathbf{k}+\mathbf{G})|^2(\mathbf{k}+\mathbf{G})_\alpha(\mathbf{k}+\mathbf{G})_\beta + \frac{1}{2}4\pi e^2 \sum_{\mathbf{G}}' \frac{|\rho(\mathbf{G})|^2}{G^2}\left[\frac{2G_\alpha G_\beta}{G^2}-\delta_{\alpha\beta}\right]$$

$$+\delta_{\alpha\beta}\sum_{\mathbf{G}}[\epsilon_{\text{xc}}(\mathbf{G})-\mu_{\text{xc}}(\mathbf{G})]\rho^*(\mathbf{G}) - \sum_{\mathbf{G},\tau}' S_\tau(\mathbf{G})\left[\frac{\partial V_\tau^L(G)}{\partial(G^2)}2G_\alpha G_\beta + V_\tau^L(G)\delta_{\alpha\beta}\right]\rho^*(\mathbf{G})$$

$$+\sum_{\mathbf{k},\mathbf{G},\mathbf{G}',i,l,\tau} S_\tau(\mathbf{G}-\mathbf{G}')\frac{\partial \Delta V_{l,\tau}^{\text{NL}}(\mathbf{k}+\mathbf{G},\mathbf{k}+\mathbf{G}')}{\partial \epsilon_{\alpha\beta}}\Psi_i(\mathbf{k}+\mathbf{G})\Psi_i^*(\mathbf{k}+\mathbf{G}') - \delta_{\alpha\beta}\left[\sum_\tau \alpha_\tau\right]\left[\Omega^{-1}\sum_\tau Z_\tau\right] + \Omega^{-1}\frac{\partial \gamma_{\text{Ewald}}}{\partial \epsilon_{\alpha\beta}}.$$

$$(2)$$

The explicit forms of the nonlocal and γ_{Ewald} terms are given in Appendixes A and B, respectively. This expression is essentially the Fourier transform of Eq. (30) of I with the Coulomb terms grouped into a properly defined form and the ion-electron term explicitly separated into $\mathbf{G}=0$ term[28] involving α_τ, plus the $\mathbf{G}\neq0$ term.

III. CALCULATIONAL METHOD

The present work employs *ab initio* normconserving pseudopotentials of the Hamann-Schlüter-Chiang[26] type, which were derived from all-electron LDA calculations of the free atom. For Si we use the form derived by Bachelet

et al.[31] (employing Wigner correlation), and the potentials covering H to Pu developed recently by Bachelet *et al.*[32] (employing Ceperley-Alder correlation) are used for Ge and GaAs. In the latter cases we use the $l = 2$ potentials as the local potentials, since this is the most consistent procedure for high angular momenta, and it furthermore makes the local as well as nonlocal potentials significantly weaker than with the choice suggested in Ref. 32.

A large number of plane waves (≈ 550) are used in all calculations, corresponding to $\hbar^2/2m\,(\mathbf{k}+\mathbf{G})^2 \leq 24$ Ry kinetic energy, in order to eliminate computational uncertainties due to cutoffs. This large cutoff is necessary with the present potentials which are relatively hard core, in order to achieve the high accuracy needed to compare reliably calculated values of elastic constants, etc., with experimental values that are known with great precision. The plane waves of high energy (> 12 Ry for Si, > 16 Ry for Ge and GaAs) are treated by second-order Löwdin perturbation theory.[33,4] The Löwdin-wave cutoffs were chosen by a test starting from no Löwdin waves and lowering the cutoff to the minimum required for reproducing accurately the all-exact-waves calculation. In the noncubic lattices suffering large strains the basis includes the same plane waves as in the undistorted crystal, i.e., we apply an ellipsoidal cutoff instead of a spherical one.

The Brillouin zone (BZ) $\mathbf{k}$ integration is performed by the special-points method of Chadi and Cohen[34] and Monkhorst and Pack,[35] suitably generalized for distorted lattices: The set of undistorted $\mathbf{k}$ points is strained $[\mathbf{k} \to (1 + \epsilon)^{-1}\mathbf{k}]$ and the symmetry of the strained lattice is used to identify equivalent $\mathbf{k}$ points. This procedure assures a smooth transition from high- to low-symmetry lattices. For Si we use the sets of two and ten special $\mathbf{k}$ points in the irreducible fcc BZ, as noted. From these calculations we estimate the error introduced by using the smaller set of special points to be $< 1\%$ for the lattice constant and $\approx 5\%$ for the elastic constants. Tests show that going beyond 10 special $\mathbf{k}$ points has neglegible effect on the calculated quantities. For Ge and GaAs we have used only two special $\mathbf{k}$ points, since their pseudopotentials require a larger numerical effort than the one used for Si.

Self-consistency is achieved with a simple mixing-coefficient scheme[36] (with $\alpha = 0.5$). A very good initial guess for the screening in a distorted structure is given by adding the screening potential plus the difference in ionic potentials (screened linearly) from some reference structure whose self-consistent screening potential is already known. Five self-consistent cycles are then usually sufficient to converge total energy, force, and stress to within 10^{-5} eV, 10^{-8} dyn, and 10^{-3} kbar, respectively. When evaluating expressions in succeeding cycles of self-consistency, it is important that all quantities refer to the same cycle. For example, when using the sum of eigenvalues in a modified version of Eq. (1),[28] the input potential energy should be subtracted and the output potential energy added to the sum of eigenvalues.

A consistency check has been performed by comparing the pressure P calculated from Eq. (2) with the derivative $-\partial E_{\text{tot}}/\partial\Omega$, obtained from values of $E_{\text{tot}}(\Omega)$ calculated from Eq. (1). It follows from the derivation of Eq. (2)

that these quantities should be equal if the basis set is held fixed for the calculations at different volumes. This holds even if the basis is not complete. In our case this means that the finite set of reciprocal-lattice vectors used in each calculation is specified by the same set of integers times the primitive vectors of the reciprocal lattice. To determine the derivatives we fit the calculated energies with the empirical Murnaghan equation of state,[37]

$$\frac{\Omega}{\Omega_0} = \left[1 + P\frac{B'}{B}\right]^{-1/B'}, \tag{3}$$

where Ω_0 denotes the equilibrium volume, B is the bulk modulus, and B' its pressure derivative $\partial B/\partial P$. With a constant number of plane waves corresponding to $|\mathbf{k}+\mathbf{G}|^2 < 32(2\pi/a)^2$ (≈ 12 Ry for a near the equilibrium value) and two special $\mathbf{k}$ points, E_{tot} and P were calculated for Si for several lattice constants between 5.25 Å and 5.60 Å. Fitting with Eq. (3) leads to the result that E_{tot} and P agree to within the numerical accuracy of the calculation, since, for example, the derived lattice constants are 5.3697 and 5.3695 Å, respectively.

On the other hand, if the basis set is not complete and is different for different volumes, the slope of the calculated energy versus volume will not equal the pressure given by Eq. (2). For example, with a constant *energy cutoff* of 12 Ry for all lattice constants, the equilibrium lattice constants deduced from E_{tot} ($a = 5.45$ Å) and P ($a = 5.36$ Å) differ by 2%, since the number of plane waves varies significantly with the lattice constant. A constant-energy cutoff may be the physically most realistic one, and 2% uncertainty in lattice constant may be sufficient in certain cases,[29] but for elastic properties greater accuracy is needed, however. For example, the bulk modulus B has an uncertainty $\Delta B/B = 3(\partial B/\partial P)(\Delta a/a)$, which is an order of magnitude larger than the fractional error in a, since $\partial B/\partial P \approx 4$. With the cutoff of 24 Ry used in the work described below, the basis set is sufficiently near completeness that the difference $\Delta a/a$ is reduced to $< 0.2\%$. We believe this is a good estimate for our numerical uncertainty in a, so that at this cutoff the corresponding uncertainty in B is $< 3\%$.

IV. STRUCTURE AND CHARGE DENSITY OF Si, Ge, AND GaAs

The equilibrium structure is the diamond structure for Si and Ge, and the zinc-blende structure for GaAs, as was verified in recent theoretical work.[29,38] With the given structure as the only input, we have calculated the lattice constant a using the stress expression Eq. (2). A first calculation of pressure at a guessed lattice constant permits a very good final estimate of a using an estimated bulk modulus. Two calculations of pressure near this value give by linear interpolation the final lattice constant where $P = 0$, as well as the bulk modulus from the slope of pressure. The results are given in Table I, showing good agreement with experiments. The deviations are state-of-the-art accuracy, and are believed to be due mainly to the local-density approximation, since our results agree well with all-electron linear-muffin-tin-orbital–atomic-

TABLE I. Lattice constants a, bulk moduli B, elastic constants c_{ij} of Si, Ge, and GaAs. The "bare" elastic constant $c_{44}^{(0)}$ [cf. Eq. (9)], the optical Γ-phonon frequency, and the internal strain parameter ζ.

| | Si | | Ge | | GaAs | | |
	Calc.	Expt.	Calc.	Expt.	Calc.	Expt.	Units
a	5.400	5.431[a]	5.59	5.65[a]	5.55	5.642[a]	Å
B	0.93	0.992[b]	0.72	0.768[b]	0.73	0.784[c]	Mbar
c_{11}	1.59	1.675[b]	1.30	1.315[b]	1.23	1.223[c]	Mbar
c_{12}	0.61	0.650[b]	0.45	0.494[b]	0.53	0.571[c]	Mbar
c_{44}	0.85	0.801[b]	0.63	0.684[b]	0.62	0.600[c]	Mbar
$c_{44}^{(0)}$	1.11		0.77		0.75		Mbar
ω_Γ	15.64	15.68[d]	9.05	9.11[e]	8.09	8.187[f]	THz
ζ	0.53	0.73(4)[g]	0.44(2)	0.72(4)[h]	0.48(2)	0.76[i]	

[a]J. Donohue, *The Structures of the Elements* (Wiley, New York, 1974).
[b]H. J. McSkimin, J. Appl. Phys. **24**, 988 (1953); H. J. McSkimin and P. Andreatch, Jr., *ibid.* **35**, 3312 (1964).
[c]C. W. Garland and K. C. Park, J. Appl. Phys. **33**, 759 (1962).
[d]T. R. Hart, R. L. Aggarwal, and B. Lax, Phys. Rev. B **1**, 638 (1970).
[e]G. Nilsson and G. Nelin, Phys. Rev. B **3**, 364 (1971).
[f]A. Mooradian and G. B. Wright, Solid State Commun. **4**, 431 (1966).
[g]References 50 and 51.
[h]C. S. G. Cousins, L. Gerward, K. Nielsen, J. Staun Olsen, B. Selsmark, B. J. Sheldon, and G. E. Webster, J. Phys. C **15**, L651 (1982).
[i]C. N. Koumelis, G. E. Zardas, C. A. Londos, and D. K. Leventuri, Acta Crystallogr. A **32**, 84 (1975).

sphere-approximation (LMTO-ASA) calculations.[39] The present results for a,B also agree with other pseudopotential calculations to within calculational uncertainties due to plane-wave cutoffs and slightly different pseudopotentials.[29,38,40]

The electronic charge density ρ is itself a physical observable which can be studied by x-ray or γ diffraction. It is, however, necessary to add the core density to the valence pseudodensity before performing comparisons. One possibility is simply to add the core density from an all-electron LDA calculation of the free atom, but this scheme is not exact when applied to the free atom itself. We suggest a scheme which assumes only the frozen-core approximation: A *deformation density* is defined as the solid pseudodensity, $\rho_{\text{solid,ps}}$, minus the density of overlapping neutral pseudoatoms, $\rho_{\text{atom,ps}}$. This density describes all effects of forming a solid out of free atoms, provided the atomic cores are frozen, in which case it should be identical to that from an all-electron calculation. Then the total solid charge density is obtained by adding overlapping all-electron atoms, ρ_{atom}, i.e.,

$$\rho_{\text{solid}} = \rho_{\text{atom}} + (\rho_{\text{solid,ps}} - \rho_{\text{atom,ps}}) . \qquad (4)$$

We believe this to be the most consistent scheme within the pseudopotential approximation.

Figure 1(a) gives the total charge density of Si in the plane of the zigzag chain along [110], using an atomic $s^2 p^2$ configuration. A double-peak or dumbbell structure is seen in the bonding region, which is present also in the valence pseudodensity (not shown). This is solely a geometric effect due to overlapping atoms, however, as is seen from Fig. 1(b) which displays the deformation density $\rho_{\text{solid,ps}} - \rho_{\text{atom,ps}}$. Almost spherical bond charges are found to cover large regions around the atomic bonds, representing an increase of up to 50% in the charge density relative to overlapping free atoms. The bond charge is

accumulated from the back-bond region in particular, as well as from the interstitial "holes" in the diamond lattice. The small accumulation in the top center of Fig. 1(b) is due to another perpendicular atomic zigzag chain. Figure 1 thus reveals the well-known effect of covalent bonding: Charge moves to the interatomic sites to screen the ionic Coulomb repulsion. A similar picture is found for Ge and GaAs.

The x-ray form (or structure) factors F_G can in many cases be related to the total electron density.[41] In the adiabatic and harmonic approximation the relation is $F_G = \rho(G) \exp[-W(G)]$, where the exponential denotes
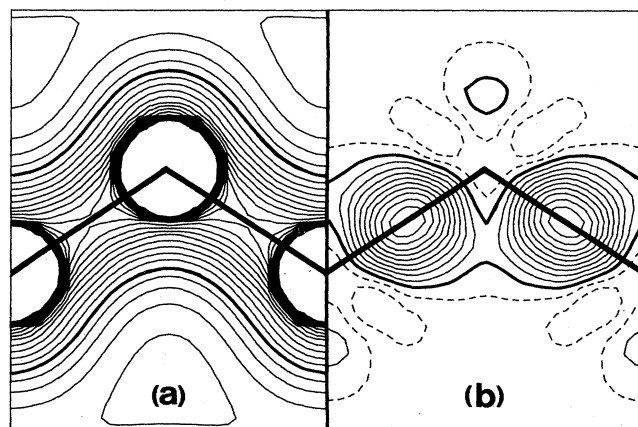
FIG. 1. (a) Total charge density [cf. Eq. (4)] of Si at the equilibrium volume, displayed in the (110)-(001) plane which contains a zigzag atomic chain. The thick contour indicates the average valence-electron density (eight electrons per cell), and the contour steps are 20% hereof. (b) The deformation density $(\rho_{\text{solid,ps}} - \rho_{\text{atom,ps}})$. The thick contour denotes zero, and the steps are 10% of the average valence-electron density. Dashed contours correspond to negative values.

the Debye-Waller factor. When the crystal consists of a single species of symmetry-related atoms (such as in the diamond structure), the Debye-Waller factor is determined by the atomic mean-square amplitude of vibration. This is also the case when $\rho(\mathbf{G})$ is assumed to consist of overlapping free-atom densities, an approximation whose quality increases for longer $\mathbf{G}$ vectors whose $F_\mathbf{G}$ are more sensitive to the details of the atomic cores. For the present crystals, Si and Ge Debye-Waller factors are given at high temperatures $(T \gg \Theta_D/6)$ in terms of the Debye temperatures Θ_D.[42,43] The case of GaAs requires some approximation for deriving $\rho(\mathbf{G})$ from experimental $F_\mathbf{G}$. We have taken the average Ga and As mean-square amplitudes (which are very similar)[43] in the Debye-Waller factor.

Table II lists the value $\rho(\mathbf{G})$ given by Eq. (4), together with experimental $\rho(\mathbf{G})$ obtained from $F_\mathbf{G}$ by dividing by the Debye-Waller factor. For GaAs the complex phase angle of $\rho(\mathbf{G})$ is also listed. The deviations are of order 1% for short $\mathbf{G}$ vectors increasing to 3% for the longer ones. The core is less accurately described than the valence electrons owing to the pseudopotential as well as local-density approximations. The present results agree to within a few percent with those of Raccah et al.,[44] Zunger,[45] Yin and Cohen,[29] and Wang and Klein.[46]

V. ELASTIC PROPERTIES OF Si, Ge, AND GaAs

Calculation of the full stress tensor is a method ideally suited to the derivation of elastic constants. The sym-

metric elastic-constant tensor has one to six independent elements, depending on the crystal symmetry. These can easily be determined from the stress calculations described here. To find the same information from the total energy would require extensive calculations. The c_{11} and c_{12} elastic constants can be found from the stress-strain relation with the application of an ϵ_1 strain. (The Voigt notation is used, i.e., $11 \rightarrow 1$, $22 \rightarrow 2$, $33 \rightarrow 3$, $23 \rightarrow 4$, $13 \rightarrow 5$, $12 \rightarrow 6$; thus $\epsilon_{11} = \epsilon_1$, $\epsilon_{23} = \frac{1}{4}\epsilon_4$, $\sigma_{11} = \sigma_1$, and $\sigma_{23} = \sigma_4$. See, e.g., Ref. 47.) This strain scales the x dimension by $(1 + \epsilon_1)$ while maintaining the y and z dimensions. By symmetry there are no internal displacements in the present lattices for any ϵ_1. For small strains the harmonic approximation defines the relations $c_{11} = \sigma_1/\epsilon_1$, $c_{12} = \sigma_2/\epsilon_1$ with the strains and stresses depicted in Fig. 2(a).

With a strain of $\epsilon_1 = -0.004$ we obtain the c_{11} and c_{12} given in Table I. The differences from experiment are -6% for Si, and up to -9% for Ge and GaAs. For Si, we used 10 special $\mathbf{k}$ points (20, in the strained crystal), whereas for Ge and GaAs only two (three, respectively) special $\mathbf{k}$ points are used, resulting in slightly lower accuracy as estimated above. These numbers agree well with the independently calculated bulk moduli $B = (c_{11} + 2c_{12})/3$. The shear modulus $\frac{1}{2}(c_{11} - c_{12})$ was given previously for Si by Wendel and Martin[4] (0.54 Mbar), and for Si (0.54 Mbar) and Ge (0.37 Mbar) by Yin and Cohen,[29] by calculating the total energy under large volume-conserving strains and fitting the energy curve with an assumed equation-of-state, in reasonable agree-

TABLE II. Fourier components $\rho(\mathbf{G})$ (in electrons per unit cell) of the total charge density of Si, Ge, and GaAs at their equilibrium volumes. The atoms are at positions $\pm(1,1,1)a/8$. Experimental data from x-ray and γ diffraction, divided by the Debye-Waller factor. For GaAs is given $|\rho(\mathbf{G})|$ and $\theta_\mathbf{G}$ in degrees, where $\rho(\mathbf{G}) = |\rho(\mathbf{G})| \exp(i\theta_\mathbf{G})$. The experiment measures only $|\rho(\mathbf{G})|$, and the table indicates this absolute value. (Dashes indicate values that are not available.)

G	Si Calc.	Si Expt.[a,b]	Ge Calc.	Ge Expt.[c]	GaAs Calc.	GaAs $\theta_\mathbf{G}$	GaAs Expt.[d]
111	-15.12	15.25	-38.80	39.43	38.78	-178	39.4
200	0		0		1.48	-90	—
220	-17.26	17.43	-47.10	47.46	46.94	180	47.3
311	-11.31	11.43	-31.14	31.37	31.02	178	31.6
222	0.341	0.382	0.280	0.277	1.30	79	—
400	-14.83	15.03	-40.32	40.51	40.09	180	41.3
331	10.17	10.35	27.26	27.72	27.10	2	28.1
420	0		0		1.45	90	—
422	13.31	13.55	35.67	36.11	35.42	-0	36.9
333	8.99	9.19	24.15	24.51	24.00	-3	24.9
511	9.03	9.20	24.17	—	24.01	3	25.0
442	-0.0231		-0.0057		1.56	-90	
622	-0.0053		0.0013		1.51	-90	

[a]R. Teworte and U. Bonse, Phys. Rev. B 29, 2102 (1984), reduced with the $\Theta_D = 528(1)$ K of P. F. Price, E. N. Maslen, and S. L. Mair, Acta. Crystallogr. A 34, 183 (1978).

[b]For the $F_{(222)}$, see R. W. Alkire, W. B. Yelon, and J. R. Schneider, Phys. Rev. B 26, 3097 (1982); for the temperature dependence of $F_{(442)}$ and $F_{(622)}$, see J. Z. Tischler and B. W. Batterman, Phys. Rev. B 30, 7060 (1984).

[c]T. Matsushita and K. Kohra, Phys. Status Solidi B 24, 531 (1974), reduced with the $\Theta_D = 290(5)$ K of B. W. Batterman and D. R. Chipman, Phys. Rev. 127, 690 (1962), and with $\Delta f' = -1.31$.

[d]T. Matsushita and J. Hayashi, Phys. Status Solidi A 41, 139 (1977), reduced as described in the text using $\Theta_{Ga} = 278(10)$ K and $\Theta_{As} = 237(10)$ K from O. H. Nielsen, F. K. Larsen, S. Damgaard, J. W. Petersen, and G. Weyer, Z. Phys. B 52, 99 (1983), and with $\Delta f'_{Ga} = -1.354$, $\Delta F'_{As} = -1.011$.
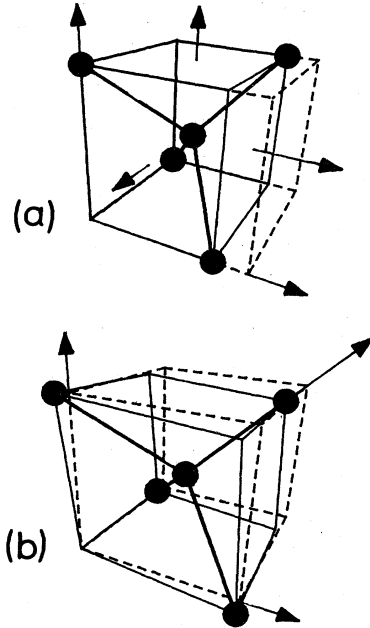
FIG. 2. Perspective view of cubes (dashed lines) deformed by strains to take new shapes (solid lines). Thick arrows indicate the resulting directions of stress exerted by the solid. (a) A strain $\epsilon_1 < 0$ along [100] resulting in σ_1 and $\sigma_2 = \sigma_3$ stresses. (b) A strain $\epsilon_4 = \epsilon_5 = \epsilon_6 < 0$ along [111] resulting in a stress in the same direction.

ment with the present results.

The calculation of the elastic constant c_{44} is inherently more complicated than that of c_{11} and c_{12}. A strain $\epsilon_4 = \epsilon_5 = \epsilon_6$ along the [111] direction [Fig. 2(b)] of a zinc-blende lattice makes the [111] atomic bond inequivalent to the other [$\bar{1}\bar{1}1$] [$\bar{1}1\bar{1}$], and [$1\bar{1}\bar{1}$] bonds. The atomic positions in the unit cell are no longer completely determined by symmetry, and a static displacement of the sublattices (the $\mathbf{k} = 0$ optical Γ phonon) is allowed. Kleinman[48] defined an internal strain parameter ζ such that the value $\zeta = 0$ corresponds to a perfect strain of atomic positions: $\mathbf{r} \rightarrow (\mathbb{1} + \epsilon)\mathbf{r}$. This is an elongation of the [111] bond by $\epsilon_4 a \sqrt{3}/4$ and of the other bonds by $1/3(\epsilon_4 a \sqrt{3}/4)$. An *actual* elongation of the [111] bond of magnitude $(1 - \zeta)\epsilon_4 a \sqrt{3}/4$ defines $\zeta = 1$ as corresponding to rigid bond lengths of $a\sqrt{3}/4$. In practice ζ is expected to fall in the range $0 < \zeta < 1$. The value of the internal strain parameter is important for many properties and has been the subject of theoretical[48,49] and experimental[50,51] work. See discussion in Appendix C. (For piezoelectric zinc-blende lattices, such as GaAs, it is necessary to specify the electrical boundary conditions. Here we calculate c_{44} and ζ for vanishing macroscopic electric fields, which is the same definition of internal strain parameter as in Ref. 49. We do not here consider the piezoelectric effect which requires the inclusion of macroscopic fields.)

In order to obtain values for ζ, c_{44}, and ω_Γ (the optical Γ-phonon frequency) the total energy of the distorted crystal can be analyzed within the adiabatic and harmonic approximations, where the energy increase per unit cell due to displacements $\mathbf{u}_\tau$ of the atoms τ in the unit cell,

and a macroscopic strain ϵ is given by

$$\Delta E_{\text{tot}} = \tfrac{1}{2} \sum_{\tau,\tau'} \mathbf{u}_\tau \Phi(\tau,\tau') \mathbf{u}_{\tau'} + \Omega \sum_\tau \mathbf{u}_\tau D(\tau)\epsilon + \tfrac{1}{2}\Omega \epsilon c^{(0)} \epsilon \ . \tag{5}$$

The force-constant matrix for atomic displacements is denoted $\Phi(\tau,\tau')$, $D(\tau)$ is related[48] to the third-rank internal strain tensor, $c^{(0)}$ is a fourth-rank tensor which gives the elastic constants in the absence of internal strain. Ω is the volume of the unstrained unit cell. Tensor contraction is understood throughout. Thus the restoring force on an atom is

$$\mathbf{F}(\tau) = - \sum_{\tau'} \Phi(\tau,\tau') \mathbf{u}_{\tau'} - \Omega D(\tau)\epsilon \ , \tag{6}$$

and the average macroscopic stress is

$$\sigma = \sum_\tau \mathbf{u}_\tau D(\tau) + c^{(0)}\epsilon \ . \tag{7}$$

The form of tensors in a cubic crystal are given by, e.g., Nye,[47] and we find for a relative atomic displacement $\mathbf{u} = u(1,1,1)$ along the [111] bond and a strain $\epsilon = \tfrac{1}{2}\epsilon_4(1 - \delta_{\alpha\beta})$ the force $\pm F(1,1,1)$ on the two atoms, where

$$F = \Phi \left[\zeta \frac{a}{4}\epsilon_4 + u \right] \ . \tag{8}$$

The force constant Φ equals $\mu \omega_\Gamma^2$, where μ is the reduced mass of the two atoms, and ω_Γ is the frequency of the transverse optic phonon at the Γ point. The stress is similarly given by $\sigma_{\alpha\beta} = \sigma_4(1 - \delta_{\alpha\beta})$ with

$$\sigma_4 = c_{44}^{(0)}\epsilon_4 + \Omega^{-1}\Phi\zeta\frac{a}{4}u \ , \tag{9}$$

where $c_{44}^{(0)}$ denotes the elastic constant that would appear in the absence of internal displacements. For a given value of ϵ_4, the actual physical displacement u is defined by $F = 0$, so that the internal displacement u equals $-\zeta a /4\epsilon_4$. Inserted into Eq. (9), this gives the stress-strain relation

$$\sigma_4 = \left[c_{44}^{(0)} - \Omega^{-1}\Phi \left[\zeta\frac{a}{4} \right]^2 \right]\epsilon_4 = c_{44}\epsilon_4 \ , \tag{10}$$

which defines the physically measured elastic constant c_{44}.

Two independent calculations now suffice to determine ω_Γ, c_{44}, and ζ. (1) With $\epsilon_4 = 0$ and a small relative displacement $u = u^{(1)}$, the force $F^{(1)}$ determines ω_Γ, from $\Phi = F^{(1)}/u^{(1)}$ and the stress $\sigma_4^{(1)}$ determines $\zeta = (4\Omega/a)\sigma_4^{(1)}/F^{(1)}$. (2) With a small $\epsilon_4^{(2)}$ and $u = 0$, the stress $\sigma_4^{(2)}$ determines $c_{44}^{(0)} = \sigma_4^{(2)}/\epsilon_4^{(2)}$, and the force $F^{(2)}$ provides an independent calculation of ζ as $4u^{(1)}F^{(2)}/a\epsilon_4^{(2)}F^{(1)}$. Thus the two force calculations determine ζ without necessarily calculating stress.

Our calculations are performed with $u^{(1)}/a = 0.002$ and $\epsilon_4^{(2)} = -0.004$, respectively, and the results are given in Table I. The phonon frequencies are within 1% of experimental values, and are in good agreement with previous calculations.[29,38] The deviations from experimental

c_{44} are of similar magnitude as for B, c_{11}, and c_{12}. The values of c_{44} are approximately 80% of $c_{44}^{(0)}$, showing that accurate calculations of the internal strain ζ are crucial to the determination of c_{44}, since ζ enters Eq. (10) as ζ^2. The two independently calculated values of ζ are consistent within $<1\%$ for Si and $<5\%$ for Ge and GaAs, and the average values are given in Table I.

The present theoretical values for ζ show interesting differences of 30—40% from those determined by analysis of two recent x-ray diffraction experiments by D'Amour et al.[50] and by Cousins et al.[51] We believe this is much larger than the calculational uncertainties in view of the accuracy obtained for all other quantities, including ω_Γ and c_{44}. Furthermore, the deformation potentials considered in Sec. VI lend independent experimental and theoretical support to the present values. Appendix C considers different theoretical approaches and discusses some possible effects upon the internal strain parameter due to nonlinearities and anharmonicity. We find that all theoretical results support the present results and that our analysis indicates that the corrections to the present values of ζ are small. Thus there persists the difference from experiment, which was also pointed out in Ref. 12. It could be speculated whether in the experiments the very low x-ray intensity of the (006) reflection is affected by multiple-scattering or extinction effects, or whether nonuniform stresses play a role. These points might be addressed in future experiments.

The charge densities of uniaxially strained crystals reveal interesting information on how electrons as well as nuclear positions respond to macroscopic strain. We consider first a strain along [100] in Si, with ϵ_1 chosen to be -0.03. Firstly the deformation density is constructed, and secondly this function is brought to the same scale as the undistorted crystal. Thirdly the deformation density of undistorted Si is subtracted. Thus Fig. 3 displays the solid's response to strain, less the term from rigidly displaced atoms. This response is to first order proportional to ϵ_1, and it is therefore quite small. However, we see clearly that the regions at roughly the midpoints between the bond charges experience a significant accumulation of charge, screening the approaching bond charges of the strained lattice. Also, a slight enhancement of the bond charges accompanies the decrease in interatomic distance.

A strain applied along the [111] axis in Si gives a quite different picture. Figure 4 displays the total charge density for a large strain $\epsilon_4 = -0.03$ (with $\epsilon_1 = -0.0073$ and $\zeta = 0.57$). Due to the internal strain it is not meaningful to subtract densities of the undistorted crystal, as was done for the [100] strain. The figure shows a relative *increase* of the bond charge on the bond oriented along [111] and a *decrease* of the bond charge along [11$\bar{1}$] (and its equivalents), compared to Fig. 1(a). To measure this charge transfer we have integrated the valence pseudo-charge contained within spheres of diameters equal to half the bond lengths. Although such spheres do not uniquely define bond charges, they do permit qualitative results. Subtracting the overlapping atom density, we find 0.1063 and 0.1003 "surplus" electrons in the left- and right-hand bond charges in Fig. 4, respectively. The undistorted density of Fig. 1(b) contains 0.1020 surplus electrons in every bond charge. Thus the three weakened bond charges are roughly compensated by the strengthened fourth bond
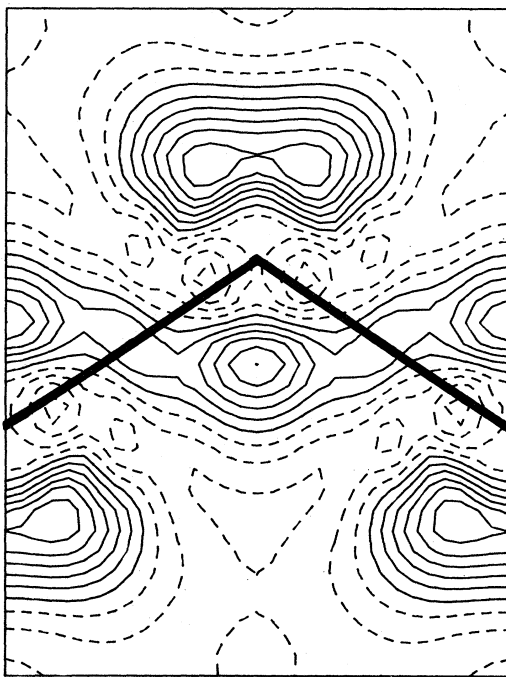
FIG. 3. Si with a strain $\epsilon_1 = -0.03$. The function plotted is the deformation density of strained Si minus the deformation density of unstrained Si, after the strained crystal has been brought to the scale of the unstrained crystal. Contour steps are 0.2% of the average valence-electron density, and dashed contours indicate negative values.
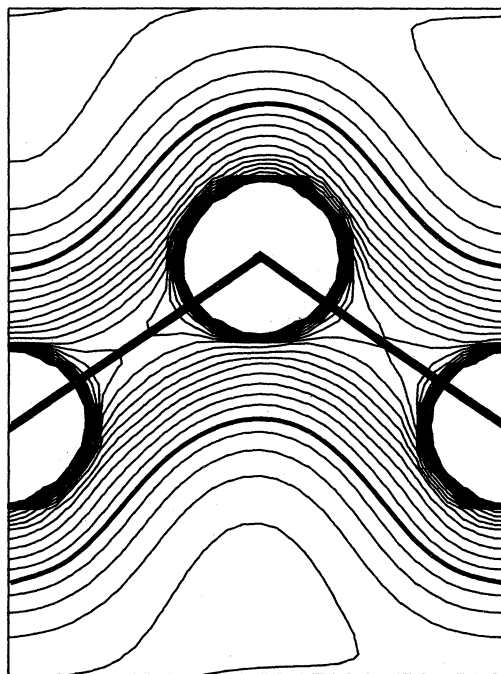
FIG. 4. Si with a strain $\epsilon_4 = -0.03$. See caption of Fig. 1(a). The left-hand bond is oriented along [111].

TABLE III. Terms in the elements of the stress tensor (in units of kbar) for Si at the theoretical lattice constant (Table I). The columns give results for undistorted Si, and with strains ϵ_1 along [100], and $\epsilon_4 = \epsilon_5 = \epsilon_6$ along [111].

	Undistorted σ_1	$\epsilon_1 = -0.004$ $\Delta\sigma_1(\propto c_{11})$	$\epsilon_1 = -0.004$ $\Delta\sigma_2(\propto c_{12})$	$\epsilon_4 = -0.004$ $\zeta = 0.51$ $\sigma_4(\propto c_{44})$
Kinetic	2243.83	16.32	11.52	2.99
Ion-electron	1452.45	24.27	4.75	−7.61
Hartree	196.06	−1.79	1.19	2.40
Ewald	−3118.06	−28.37	−11.09	5.22
Exchange-correlation	−774.10	−3.89	−3.89	0
Total	0.18	6.54	2.48	3.00

charge around each atom, although other charge transfers are evident from Fig. 4 as well. We find that bond charges adjust to screen approaching ions, a picture that holds also for an optical Γ-phonon displacement which has the same symmetry as the lattice strained along [111]. The same picture was previously found for the TO(Γ) phonon by Wendel and Martin,[4] Yin and Cohen,[29] and Resta and Baldereschi.[52]

It is interesting to break down the stresses into separate contributions according to Eq. (2). This is given in Table III for σ_1 and $\sigma_2 = \sigma_3$ resulting from an ϵ_1 strain, and for σ_4 resulting from an ϵ_4 strain. For both σ_1 and σ_2 the Ewald term is negative, indicating the instability towards collapse that results from the attractive ion-background interaction. The negative contribution to the shear $\sigma_1 - \sigma_2$ is a consequence of the strong repulsion between the nearest neighbors. The increase of kinetic energy results from the compression and is greater in the 1 or x direction. The ion-electron interactions are positive and are the most important terms in stabilizing the solid against shear, i.e., in making $\sigma_1 - \sigma_2$ positive. This latter effect is a clear manifestation of the directional covalent bonding which is necessary for the shear stability of the diamond structure.

The contributions to the stress have very different character for the off-diagonal shear stress σ_4. The signs of each term except the kinetic one is opposite to that for the other shear stress $\sigma_1 - \sigma_2$. We believe that this qualitative difference results from the inequivalence of the bonds and the associated internal strain in the case of σ_4 stress. The balance of the repulsive nearest-neighbor ion-ion terms and the bonding electronic terms is different leading to different individual contributions. The total is, nevertheless, comparable. It is interesting to note that in this case the negative ion-electron stress is almost exactly compensated by the Ewald and Hartree repulsion so that the total stress is close to the value of the kinetic stress.

VI. DEFORMATION POTENTIALS IN Si

The indirect optical gap of Si occurs between the valence-band maximum at $k = 0$ ($\Gamma_{25'}$ state) and a conduction-band minimum near the X point.[53] Application of strain shifts and sometimes splits these states. To first order in the strain this effect is described in terms of *deformation potential* parameters, as discussed in detail by Laude, Pollak, and Cardona.[53] All parameters may be

found by applying [100] and [111] strains. The present work considers the splitting of the $\Gamma_{25'}$ state, yielding the b, d, d', and d_0 deformation potentials. The spin-orbit interaction can be neglected without causing any problems, since it is relatively insensitive to the applied strain.[53] Although the local-density eigenvalues do not represent well the physical energies (see discussion of Sham and Schlüter[54]), the fractional errors are small relative to the overall scale of bandwidths and we can expect the deformation potentials to be accurate on the level of order 10%, to which they are known experimentally.

The definitions of Laude *et al.* lead to the following expressions for the $\Gamma_{25'}$ splitting:

$$\Delta E^{(100)} = 3b(\epsilon_1 - \epsilon_2) , \tag{11a}$$

$$\Delta E^{(111)} = \tfrac{3}{2}\sqrt{3}d\epsilon_4 \tag{11b}$$

for [100] and [111] strains, respectively, thereby defining b and d in the absence of spin-orbit splitting. Due to the internal-strain degree of freedom, d may be decomposed into a pure-strain ($\zeta = 0$) part d' and a phonon part d_0 as[55]

$$d = d' - \tfrac{1}{4}\zeta d_0 , \tag{11c}$$

with ζ defined as in the preceding section.

With a [100] strain $\epsilon_1 = -0.03$ (using two fcc special k points) we calculate b in good agreement (Table IV) with the optical-absorption experiments of Laude *et al.*[53] A [111] strain $\epsilon_{4-6} = -0.004$ and $\epsilon_{1-3} = -0.001$ and several values of ζ give the d, d', and d_0 in Table IV. The linearity assumption of Eq. (11c) is well fulfilled. Independent calculations have recently been performed by Christensen[56] using the relativistic LMTO-ASA method both with and without spin-orbit interaction (Table IV). References to earlier work may be found in that paper. Although the two methods solve the local-density Schrödinger equation by different methods, very close answers are found for b, and for d with values of ζ around 0.5, whereas d_0 differs somewhat. Christensen does not calculate ζ directly, but in view of the experimental d values (Table IV) he concludes that $\zeta \approx 0.4$—0.6. If the experimental value of $\zeta = 0.73$ (Table I) is assumed, the calculated d will be about −7 eV, in sharp disagreement with experimental d. Thus the experimental deformation potentials are found to support a value of ζ close to the present theoretical value of 0.53, rather than the experimental ζ of Refs. 50 and 51.

TABLE IV. Band-splitting parameters, or deformation-potential parameters, of Si [cf. Eq. (11)] in units of eV. The values of d correspond to the internal strain ζ indicated in parenthesis. Furthermore, the optical Γ-phonon-splitting parameters s_{100} and s_{111}, and mode-Grüneisen parameter γ [cf. Eqs. (12) and (13)].

	Present work	Christensen[a]	Expt.
b	-2.28	-2.270	$-2.10(10)^{b}$
d	-5.47	-5.29	$-4.85(15)^{b}$
	($\zeta=0.53$)	($\zeta=0.50$)	
d_0	29.83	22.7	26.6^{c}
d'	-1.52	-2.46	—
s_{100}	0.131		0.24^{d}
s_{111}	-0.90		$-0.93(5)^{d}$
γ	0.9		0.98^{e}

[a]Reference 56.
[b]Reference 53.
[c]C. Jacoboni, G. Gagliani, L. Reggiani, and O. Turci, Solid State Electron. 21, 315 (1978).
[d]Reference 57.
[e]B. A. Weinstein and G. J. Piermarini, Phys. Rev. B 12, 1172 (1975).

VII. STRAIN-SPLITTING OF THE TO(Γ) PHONON

The threefold degenerate optic-phonon modes at $\mathbf{k}=0$ (Γ) of the diamond structure are split when uniaxial strain lowers the symmetry of the crystal. One mode is polarized parallel to the strain and the remaining two are perpendicularly polarized. This effect is due to inequivalent force-constant changes in the three directions. We consider the case of a strain along [100] with phonons polarized along [100] and [001], respectively, and the case of a strain along the [111] direction, and calculate the phonons polarized along [111] and [11$\bar{2}$], respectively.

Since the splitting is small (proportional to strain), care must be taken to minimize the effect of anharmonicity. By choosing both positive and negative displacements for strain along [111] the third-order anharmonicity is canceled, whereas the fourth-order term is negligible for the present small displacements. We define the phonon-splitting parameters s_{100} and s_{111} by

$$\Delta\omega_\Gamma = \omega_\Gamma[100] - \omega_\Gamma[001] = s_{100}\omega_\Gamma(\epsilon_1 - \epsilon_2) , \quad (12a)$$

$$\Delta\omega_\Gamma = \omega_\Gamma[111] - \omega_\Gamma[11\bar{2}] = s_{111}\omega_\Gamma\epsilon_4 , \quad (12b)$$

respectively, where the brackets denote polarization direction. A calculation with $\epsilon_4 = -0.004$ (and $\epsilon_1 = -0.001$; two fcc special $\mathbf{k}$ points), and one with $\epsilon_1 = -0.004$ give the values shown in Table III. The value s_{111} is in good agreement with the optical data of Chandrasekhar et al.,[57] but the s_{100} is only one-half of the experimental value.

In addition to the splitting, a shift $\Delta\omega_h$ of the center of gravity of the three phonon modes occurs owing to the hydrostatic component of the strain. The first-order shift is

$$\Delta\omega_h = -3\gamma\omega_\Gamma\epsilon_1 , \quad (13)$$

where γ defines the mode Grüneisen parameter. Of course, this parameter can be most easily calculated by changing the volume and this has been done by Yin and Cohen.[29] Here we extract this information only as a check on our present lower-symmetry calculations. The strain ϵ_1 is to first order given by $c_{44}\epsilon_4/3B$. From $\epsilon_4 = -0.004$ we find $\gamma = 0.7$, and from $\epsilon_4 = -0.03$ we find $\gamma = 0.9$. We estimate these values to be calculated to within $\approx 20\%$, most accurately for the strain $\epsilon_4 = -0.03$. This value agrees satisfactorily with experiment (Table IV), and with the more accurate calculation by Yin and Cohen[29] which was aimed at obtaining γ.

VIII. NONLINEAR ELASTIC PROPERTIES

Elastic properties beyond the harmonic approximation are conveniently described by the stress method. For large strains it is customary to Taylor-expand the total energy using Lagrangian strains $\eta_{\alpha\beta}$, with the coefficients thereby defining higher-order elastic constants.[58] If ϵ is the usual strain tensor, η is defined by

$$\eta = \epsilon + \tfrac{1}{2}\epsilon^2 . \quad (14)$$

Both $\underline{\epsilon}$ and η are symmetric (rotation free). The Lagrangian stress $t_{\alpha\beta} = \partial E_{\text{tot}}/\partial\eta_{\alpha\beta}$ is defined from the usual stress $\sigma_{\alpha\beta}$ by

$$t = \det(1+\epsilon)(1+\epsilon)^{-1}\sigma(1+\epsilon)^{-1} . \quad (15)$$

We consider two types of large strains. Firstly, a strain ϵ_1 which scales only the x direction of the crystal, leading to the fourth-order expansion of stress:

$$t_1 = c_{11}\eta_1 + \tfrac{1}{2}c_{111}\eta_1^2 + \tfrac{1}{6}c_{1111}\eta_1^3 , \quad (16a)$$

$$t_2 = t_3 = c_{12}\eta_1 + \tfrac{1}{2}c_{112}\eta_1^2 + \tfrac{1}{6}c_{1112}\eta_1^3 , \quad (16b)$$

where $\eta_1 = \epsilon_1 + \tfrac{1}{2}\epsilon_1^2$. Secondly, for a combination of strain along the [111] direction ($\epsilon_4 = \epsilon_5 = \epsilon_6$) and a volume scaling ($\epsilon_1 = \epsilon_2 = \epsilon_3$), the third-order expansion of stress is

$$t_1 = t_2 = t_3 = (c_{11} + 2c_{12})\eta_1 + \tfrac{1}{2}(c_{111} + 6c_{112} + 2c_{123})\eta_1^2$$
$$+ \tfrac{1}{2}(c_{144} + 2c_{166})\eta_4^2 , \quad (17a)$$

TABLE V. Higher-order elastic properties of Si. Third- and fourth-order constants, pressure derivative of bulk modulus, $\partial B/\partial P$, and rates of change of internal strain ζ with macroscopic strain stains. Experimental data: H. J. McSkimin and P. Andreatch, Jr., J. Appl. Phys. 35, 3312 (1964).

	Calc.	Expt.	
c_{111}	-7.5	$-8.25(10)$	Mbar
c_{112}	-4.8	$-4.51(5)$	Mbar
c_{123}	≈ 0	$-0.64(10)$	Mbar
$c_{144} + 2c_{166}$	-5.8	$-6.08(20)$	Mbar
c_{456}	-0.8	$-0.64(20)$	Mbar
$\partial B/\partial P$	3.8	4.15	
c_{1111}	≈ 0	—	Mbar
c_{1112}	32	—	Mbar
$\partial\zeta/\partial\epsilon_1$	-4.5	—	
$\partial\zeta/\partial\epsilon_4$	-1.3	—	
$\partial\zeta/\partial\epsilon_4\vert_{\text{expt}}$	-2.7	—	

TABLE VI. Total energy and pressure of Si as a function of lattice constant (using 10 fcc special **k** points) relative to the value of $E_{tot} = -215.6638$ eV at $a = 5.400$ Å.

a (Å)	ΔE_{tot} (eV)	P (kbar)
5.40	$\equiv 0$	$\equiv 0$
5.30	0.0453	59.6
5.20	0.1774	135.1
5.10	0.4099	229.8
5.00	0.7625	347.5

$$t_4 = t_5 = t_6 = c_{44}\eta_4 + (c_{144} + 2c_{166})\eta_1\eta_4 + c_{456}\eta_4^2 \ . \quad (17b)$$

The pressure derivative $\partial B/\partial P$ of the bulk modulus B is from Eq. (17a) given by

$$\partial B/\partial P = -(c_{111} + 6c_{112} + 2c_{123})/9B \ . \quad (18)$$

First, we calculate energy and pressure for Si, using 10 fcc special **k** points, as a function of lattice constant $(5.25 < a < 5.60 \text{ Å})$. This corresponds to $\eta_1 \neq 0$ and $\eta_4 = 0$ in Eq. (17), and fitting yields $B = 0.95$ Mbar in good agreement with Table I, and $\partial B/\partial P$ as given in Table V. The value differs slightly from Ref. 20, which used the equation-of-state Eq. (3) instead of Eq. (12). The actual values of E_{tot} and P are interesting both for studying phase transitions,[17,24] and for comparison with other calculations, and the values are listed in Table VI.

Second, the σ_1 and $\sigma_2 = \sigma_3$ stresses are calculated (using the equivalent of two fcc special **k** points) for a uniaxial [100] strain with $-0.1 < \epsilon_1 < +0.03$. Using Eq. (16) the third-order elastic constants c_{111} and c_{112}, and the fourth-order ones c_{1111} and c_{1112}, are found. Fairly good agreement ($<10\%$ error) with experiment[58] is found for c_{111} and c_{112}, whereas c_{1111} and c_{1112} have not been measured, to our knowledge. From Eq. (18) the constant c_{123} can now be deduced, but with the present accuracy we can only conclude that $c_{123} \approx 0$. Experimentally, c_{123} is close to zero (Table V).

Third, the $\sigma_1 = \sigma_2 = \sigma_3$ and $\sigma_4 = \sigma_5 = \sigma_6$ stresses are calculated for [111] strains with $-0.1 < \epsilon_4 < +0.03$, and $\epsilon_1 = -1 + (1 - \frac{1}{2}\epsilon_4^2)^{1/2}$ so that $\eta_1 \equiv 0$. We define ζ for large ϵ_4 as above, $\zeta = 4u/(a\epsilon_4)$ [cf. Eqs. (8)—(10)]. For each ϵ_4 the internal strain parameter ζ is optimized to yield zero forces on the atoms. With Eq. (17) the constants $c_{144} + 2c_{166}$ and c_{456} are derived (Table V), with fairly small deviations from experimental values. We did not calculate c_{144} and c_{166} individually, although it can in principle be done by choosing suitable strains yielding other linear combinations of these constants.

In Fig. 5 are plotted the Lagrangian stresses as functions of Lagrangian strains, corresponding to the above described calculations. The internal strain parameter ζ derived by the above procedure is displayed in Fig. 6 (dashed curve), showing significant anharmonicity at large strains. An ideal experiment applying uniaxial pressure along [111] will yield strains different from the ones used above, however. The stress tensor will be $\sigma_{\alpha\beta} = P/3$ for all α, β, where P is the external uniaxial pressure, corresponding to zero stress in the directions perpendicular to
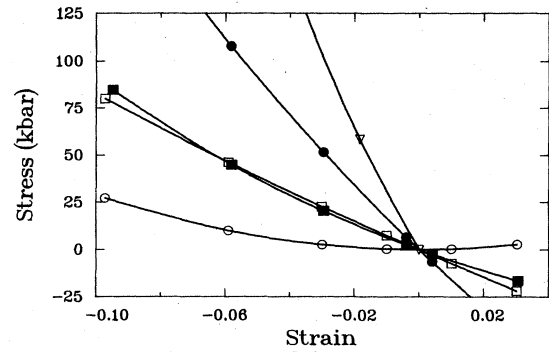
FIG. 5. Lagrangian stresses [cf. Eqs. (16) and (17)] as function of Lagrangian strains [cf. Eq. (14)]. The $\triangledown$ denote the isotropic pressure-volume relation [Eq. (17a)]. The $\bullet$ denote t_1 stresses, and $\blacksquare$ denote t_2 stresses for [100] strains [Eq. (16)]. The $\bigcirc$ denote t_1 stresses, and $\square$ denote t_4 stresses for [111] strains [Eq. (17)].

[111]. For a given ϵ_4, this requires optimizing the internal strain ζ as well as the macroscopic strain ϵ_1. Such calculations show that the volume of the crystal is further decreased, in good agreement with Eq. (17) and with the elastic constants in Table II, and that ζ increases more rapidly as displayed in Fig. 6 (solid curve). Fitting the two curves in Fig. 6 with a polynomial quadratic in ϵ_1 and ϵ_4 yields the rates of change $\partial\zeta/\partial\epsilon_1$ for $\epsilon_4 = 0$ and $\partial\zeta/\partial\epsilon_4$ for $\epsilon_1 = 0$. The rate of change that would be seen in an experiment corresponds to the solid curve in Fig. 5, where to first order $\epsilon_1 = c_{44}\epsilon_4/3B$. The rate of change of ζ are given in Table V, but are unknown experimentally. The present results predict the ζ as a function of uniaxial pressure (indicated by the top scale in Fig. 6).

Thus we find significant changes in ζ with applied pressure, up to $\Delta\zeta \approx +40\%$ at pressures $P \approx 200$ kbar. This increase makes physical sense, since large strains force the repelling cores to approach each other, and the energy can thus be lowered by an outward relaxation. However, current experimental techniques obtain uniaxial pressures
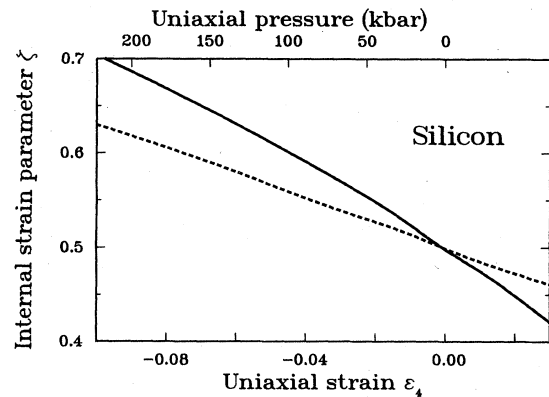
FIG. 6. Internal strain parameter ζ as function of [111] strain ϵ_4. The solid curve is derived for zero transverse pressure, corresponding to experimental conditions. The uniaxial pressure indicated on the top axis refers to this case, only. The dashed curve gives ζ when $\eta_1 = 0$ in Eq. (17), as derived from the calculations of elastic constants.

in the 10—15-kbar range, where ζ is changed only by a few percent. Large uniaxial pressures are experimentally unattainable at present, and a hydrostatic pressure of about 125 kbar will transform cubic Si to the metallic β-tin structure. Phase transitions of Si under uniaxial pressure have not been reported, to the authors' knowledge.

IX. CONCLUSION

We have given explicit local-density-functional expressions for the stress tensor in a form for evaluation in reciprocal space. This result is based upon the stress theorem given previously by the authors, and is the Fourier transform of the real-space expression given in I. Calculations were performed with *ab initio* normconserving pseudopotentials as parametrized by Bachelet *et al.*[31,32] With large basis sets it was possible to obtain full convergence of total energy, force, and stress. We studied the lattice constants, bulk moduli, elastic constants, Γ-phonon frequencies, and x-ray form factors and found very good agreement with experiment. The internal strain parameter ζ deviates strongly from that found in x-ray diffraction experiments, but our values are supported by comparing calculated deformation potentials with experimental ones. An independent calculation[56] of deformation potentials by the LMTO-ASA method supports our result for ζ. We also obtained the strain splitting of the Γ phonon, in good agreement with experiment for strain along [111] but only half the experimental value for strain along [100]. An almost complete set of third-order elastic constants for Si agrees well with experiment, and we present a prediction of the anharmonicity of the internal strain parameter and several fourth-order elastic constants.

In conclusion, we have established the great utility of calculating stress in addition to forces and total energy, and we have demonstrated that accurate results can be obtained for a wide variety of properties related to macroscopic distortions of perfect crystals.

APPENDIX A

The nonlocal contribution to the stress Eq. (2) is given as follows: The $(\mathbf{K}, \mathbf{K}')$ plane-wave matrix element of a nonlocal potential $V_{\tau l}^{\mathrm{NL}}$ for an atom labeled τ and for angular momentum l is[59]

$$V_{\tau l}^{\mathrm{NL}}(\mathbf{K}, \mathbf{K}') = \frac{4\pi}{\Omega}(2l + 1)P_l(\cos\theta)F_{\tau l}(K, K') , \qquad \text{(A1)}$$

where P_l is the Legendre polynomial, θ the angle between $\mathbf{K}$ and $\mathbf{K}'$, and the factor $F_{\tau l}$ is

$$F_{\tau l}(K, K') = \int_0^\infty j_l(Kr)j_l(K'r)V_{\tau l}^{\mathrm{NL}}(r)r^2 dr \qquad \text{(A2)}$$

with $j_l(x)$ denoting spherical Bessel functions. The strain derivative of Eq. (A1) with respect to $\epsilon_{\alpha\beta}$ is, using the scaling of reciprocal-space vectors,

$$\frac{\partial K_\gamma}{\partial \epsilon_{\alpha\beta}} = -\delta_{\alpha\gamma}K_\beta \qquad \text{(A3)}$$

equal to

$$\frac{\partial V_{\tau l}^{\mathrm{NL}}(\mathbf{K}, \mathbf{K}')}{\partial \epsilon_{\alpha\beta}} = \frac{4\pi}{\Omega}(2l + 1)\left\{ -\delta_{\alpha\beta}P_l(\cos\theta)F_{\tau l}(K, K') + P_l(\cos\theta)\frac{\partial F_{\tau l}(K, K')}{\partial \epsilon_{\alpha\beta}} \right.$$

$$\left. + \left[\cos\theta\left[\frac{K_\alpha K_\beta}{K^2} + \frac{K'_\alpha K'_\beta}{K'^2} \right] - \frac{(K_\alpha K'_\beta + K'_\alpha K_\beta)}{KK'} \right] P'_l(\cos\theta)F_{\tau l}(K, K') \right\} . \qquad \text{(A4)}$$

Here $P'_l(x)$ denotes the derivative of $P_l(x)$.

Several methods may be chosen to calculate the nonlocal stress. For example, if $V_{\tau l}^{\mathrm{NL}}(r)$ is expressed in terms of a Gaussian, $\exp(-r^2/R^2)$ (R being a decay length), the expression for $V_{\tau l}^{\mathrm{NL}}(\mathbf{K}, \mathbf{K}')$ is given by Heine and Weaire,[59] and the strain derivative of $F_{\tau l}$ used in Eq. (A4) is

$$\frac{\partial F_{\tau l}(K, K')}{\partial \epsilon_{\alpha\beta}} = \frac{\sqrt{\pi}}{4}R^3 e^{-R^2(K-K')^2/4}\left[(K_\alpha K_\beta + K'_\alpha K'_\beta)\tfrac{1}{2}R^2 B_l(\tfrac{1}{2}KK'R^2) \right.$$

$$\left. - \tfrac{1}{2}KK'R^2\left[\frac{K_\alpha K_\beta}{K^2} + \frac{K'_\alpha K'_\beta}{K'^2} \right][B_l(\tfrac{1}{2}KK'R^2) + B'_l(\tfrac{1}{2}KK'R^2)] \right] . \qquad \text{(A5)}$$

The function denoted $B_l(x)$ is a well-behaved function related to the modified spherical Bessel functions of the first kind $I_{l+1/2}(x)$ by

$$B_l(x) = e^{-x} \left[\frac{\pi}{2x} \right]^{1/2} I_{l+1/2}(x) \ . \tag{A6}$$

$B_l(x)$ satisfies the same recursion formulas as $I_{l+1/2}(x)$, and the first two functions are

$$B_{-1}(x) = \frac{1 + e^{-2x}}{2x} \quad \text{and} \quad B_0(x) = \frac{1 - e^{-2x}}{2x} \ . \tag{A7}$$

Alternatively, if $F_{\tau l}(K,K')$ is calculated numerically from an interpolation table, the partial derivatives are easily evaluated, and we have

$$\frac{\partial F_{\tau l}(K,K')}{\partial \epsilon_{\alpha\beta}} = -K \frac{\partial F_{\tau l}}{\partial K} \frac{K_\alpha K_\beta}{K^2} - K' \frac{\partial F_{\tau l}}{\partial K'} \frac{K'_\alpha K'_\beta}{K'^2} \ . \tag{A8}$$

APPENDIX B

The stress contribution from the ion-ion Coulomb interactions in a compensating negative background is given from the Madelung energy γ_{Ewald} which is calculated by the Ewald transformation.[30,28] The strain derivative is

$$\frac{\partial \gamma_{\text{Ewald}}}{\partial \epsilon_{\alpha\beta}} = \frac{\pi}{2\Omega\epsilon} \sum_{G\neq 0} \frac{e^{-G^2/4\epsilon}}{G^2/4\epsilon} \left| \sum_\tau Z_\tau e^{iG\cdot x_\tau} \right|^2 \left[\frac{2G_\alpha G_\beta}{G^2}(G^2/4\epsilon + 1) - \delta_{\alpha\beta} \right]$$

$$+ \tfrac{1}{2}\epsilon^{1/2} \sum_{\tau\tau' T} Z_\tau Z_{\tau'} H'(\epsilon^{1/2}D) \frac{D_\alpha D_\beta}{D^2} \bigg|_{(D = x_{\tau'} - x_\tau + T \neq 0)} + \frac{\pi}{2\Omega\epsilon} \left[\sum_\tau Z_\tau \right]^2 \delta_{\alpha\beta} \ . \tag{B1}$$

Here ϵ denotes a convergence parameter (and *not* the strain $\epsilon_{\alpha\beta}$) which may be chosen for computational performance. Z_τ denotes the atomic core charge of atom τ, T the lattice translation vectors, and x_τ the atomic positions in the unit cell. The function $H'(x)$ is

$$H'(x) = \partial[\text{erfc}(x)]/\partial x - x^{-1}\text{erfc}(x) \tag{B2}$$

with $\text{erfc}(x)$ denoting the complementary error function.

APPENDIX C

Different theoretical approaches for calculating the internal strain parameter ζ (see Sec. V) are discussed, followed by possible corrections to the simple analysis presented in Sec. V.

The earlier theoretical approaches employed empirical phonon models to fit the experimental phonon dispersion or the elastic constants. The obtained ζ values were reviewed by Cousins.[60] The most reliable phonon model for the covalent semiconductors is the adiabatic bond-charge model,[61] which gives $\zeta = 0.50$ (Si) and $\zeta = 0.52$ (Ge), in fairly good agreement with the present results. Considering the scope of empirical phonon models, their disagreement with reported experimental values of ζ has lead to limited concerns, only.

The first *ab initio* calculation of ζ was reported by Harmon *et al.*[62] for Si ($\zeta = 0.61$) using a localized Gaussian basis set to calculate total energy. A large ϵ_4 strain ($\epsilon_4 = -4.7\%$) was applied while maintaining a constant volume. They deduced ζ from a shallow minimum of total energy (their Fig. 3), which may be compared to our large-strain determinations of ζ (see Fig. 6). Their value agrees well with the present results, given their large strain ϵ_4 and the values of ζ and $\partial\zeta/\partial\epsilon_4$ in Table V. Sánches-Dehesa *et al.*[63] applied a similar procedure using

local pseudopotentials for Si and a six-atom unit cell, obtaining the values $\zeta = 0.86$ and $c_{44} = 1.2$ Mbars. In our opinion, there are inaccuracies in this calculation so that it is not a stringent test of the *ab initio* methods. Cardona *et al.*[64] used the planar force constants found by supercell calculations for GaAs (Ref. 10) and for Si (Ref. 11) (the latter calculation employed an *ad hoc* adjustment to fit frozen-phonon calculations). The values of ζ were 0.72 (GaAs) and 0.57 (Si). Using the stress method we found $\zeta = 0.65$ in GaAs with the empirical pseudopotential used in Ref. 10, showing the results of Ref. 64 to be of fair accuracy.

We conclude that the most accurate theoretical values for ζ are the ones obtained with the present stress method. These are the only calculations which are sufficiently accurate to demonstrate that the theoretical value for ζ is definitely below that which has been gotten from the analysis of experiments. Since so many other properties are given well by these *ab initio* calculations we believe the theoretical results must be taken seriously.

Notwithstanding the present results, it is necessary to address possible sources of theoretical uncertainty. For example, the harmonic approximation results are confirmed since, for the given strain ϵ_4, an internal displacement $u = \zeta a \epsilon_4/4$ yields a force F which is essentially zero. We discuss in addition several effects due to finite strains which might conceivably affect the value of ζ.

Firstly, ζ will have anharmonic contributions at large strains (Fig. 6). We have investigated this in detail for Si (see below), and find for the experimental conditions ($P < 15$ kbar) an increase in ζ of about 5% over the value of Table I, which is much smaller than the discrepancy with experiment.

Secondly, the analysis of the x-ray diffraction data as-

sumed free-atom form (structure) factors, which neglect solid-state effects on the charge density. However, for the [006] reflection used to determine ζ, we found negligible difference between the solid form factors, and the free-atom ones used by Cousins et al.[51] Furthermore, as a test we compared our calculated $\rho(\mathbf{G})$ with the analysis of Ref. 50, and found good agreement with our value of ζ as given in Table I.

Thirdly, anharmonic thermal vibrations will in general shift the atoms when the cubic symmetry is lowered by [111] strains. A cubic anharmonic energy term gives rise to a thermally averaged force $-\frac{1}{2}\Phi\langle\mathbf{uu}\rangle$, where Φ is the

third-order force-constant matrix, and $\langle\mathbf{uu}\rangle$ is a displacement correlation matrix. With Keating's[65] anharmonic force constant, which is close to that found in ab initio calculations ($\approx 3\times10^{12}$ dyn/cm^2) and a typical mean-square displacement ($\langle u_x^2\rangle\approx0.01$ Å^2), and a geometry factor proportional to the ϵ_4 strain ($\epsilon_4\approx-0.01$), a force of order $\approx10^{-8}$ dyn results. In comparison, the force resulting from Eq. (8) with $\epsilon_4=-0.01$ and $u=0$ is $\approx10^{-5}$ dyn, so that anharmonic displacement does not appear to be important. Thus we do not find any important correction terms to the theoretical calculation of ζ, and the discrepancy with experiments seems to persist.

*Present address.

[1]W. Kohn and L. J. Sham, Phys. Rev. 140, A1133 (1965); L. J. Sham and W. Kohn, ibid. 145, B561 (1966).

[2]Theory of the Inhomogeneous Electron Gas, edited by N. H. March and S. Lundqvist (Plenum, New York, 1983).

[3]V. L. Moruzzi, J. F. Janak, and A. R. Williams, Calculated Electronic Properties of Metals (Pergamon, New York, 1978).

[4]H. Wendel and R. M. Martin, Phys. Rev. Lett. 40, 950 (1978); Phys. Rev B 19, 5251 (1979).

[5]J. Ihm and M. L. Cohen, Solid State Commun. 29, 711 (1979).

[6]See, also, H. L. Skriver, The LMTO Method. Muffin Tin Orbitals and Electronic Structure (Springer-Verlag, Berlin, 1984).

[7]K.-M. Ho, C. L. Fu, and B. N. Harmon, Phys. Rev. B 29, 1575 (1984).

[8]H. J. F. Jansen and A. J. Freeman, Phys. Rev. B 30, 561 (1984).

[9]M. T. Yin and M. L. Cohen, Phys. Rev. B 26, 5668 (1982).

[10]K. Kunc and R. M. Martin, Phys. Rev. B 24, 2311 (1981); J. Ihm, M. T. Yin, and M. L. Cohen, Solid State Commun. 37, 491 (1981); K. M. Ho, C. L. Fu, and B. N. Harmon, Phys. Rev. B 28, 6687 (1983).

[11]K. Kunc and R. M. Martin, Phys. Rev. Lett. 48, 406 (1982); M. T. Yin and M. L. Cohen, Phys. Rev. B 25, 4317 (1982).

[12]O. H. Nielsen and R. M. Martin, Phys. Rev. Lett. 50, 697 (1983).

[13]See, for example, M. L. Cohen, J. Phys. Soc. Jpn. 49, 13 (1980); K. Kunc and R. M. Martin, Physica 117B, 511 (1983).

[14]H. Hellmann, Einführung in die Quantenchemie (Deuticke, Leipzig, 1937), pp. 61 and 285; R. P. Feynman, Phys. Rev. 56, 340 (1939); undergraduate thesis, Massachusetts Institute of Technology, 1939 (unpublished).

[15]P. Ehrenfest, Z. Phys. 45, 455 (1927).

[16]See, e.g., P. Pulay, in Modern Theoretical Chemistry (Plenum, New York, 1977), Vol. 4, p. 153.

[17]R. Biswas, R. M. Martin, R. J. Needs, and O. H. Nielsen, Phys. Rev. B 30, 3210 (1984).

[18]J. E. Northrup and M. L. Cohen, J. Vac. Sci. Technol. 21 333 (1982).

[19]O. H. Nielsen, R. M. Martin, D. J. Chadi, and K. Kunc, J. Vac. Sci. Technol. B 1, 714 (1983).

[20]O. H. Nielsen and R. M. Martin, Phys. Rev. B 32, 3780 (1985) (preceding paper, referred to as I).

[21]A. G. McLellan, Am. J. Phys. 42, 239 (1974).

[22]M. Born, W. Heisenberg, and P. Jordan, Z. Phys. 35, 557 (1926).

[23]V. Fock, Z. Phys. 63, 855 (1930).

[24]R. J. Needs and R. M. Martin, Phys. Rev. B 30, 5390 (1984).

[25]See, e.g., Solid State Physics, edited by H. Ehrenreich, F. Seitz, and D. Turnbull (Academic, New York, 1980), Vol. 24.

[26]D. R. Hamann, M. Schlüter, and C. Chiang, Phys. Rev. Lett.

43, 1494 (1979).

[27]G. Kerker, J. Phys. C 13, L189 (1980).

[28]J. Ihm, A. Zunger, and M. L. Cohen, J. Phys. C 12, 4409 (1979).

[29]M. T. Yin and M. L. Cohen, Phys. Rev. B 25, 7403 (1982).

[30]K. Fuchs, Proc. R. Soc. London, Ser. A 151, 585 (1935).

[31]G. B. Bachelet, H. S. Greenside, G. A. Baraff, and M. Schlüter, Phys. Rev. B 24, 4745 (1981).

[32]G. B. Bachelet, D. R. Hamann, and M. Schlüter, Phys. Rev. B 26, 4199 (1982).

[33]P. O. Löwdin, J. Chem. Phys. 19, 1396 (1951); D. Brust, Phys. Rev. 134, A1337 (1964).

[34]D. J. Chadi and M. L. Cohen, Phys. Rev. B 8, 5747 (1973).

[35]H. J. Monkhorst and J. D. Pack, Phys. Rev. B 13, 5188 (1976).

[36]R. M. Martin and K. Kunc, in Ab initio Calculation of Phonon Spectra, edited by T. Devreese, V. E. Van Doren, and P. E. Van Camp (Plenum, New York, 1983), p. 65.

[37]F. D. Murnaghan, Proc. Nat. Acad. Sci. U.S.A. 50, 697 (1944).

[38]S. Froyen and M. L. Cohen, Phys. Rev. B 28, 3258 (1983).

[39]D. Glötzel, B. Segall, and O. K. Andersen, Solid State Commun. 36, 403 (1980); A. K. McMahan, Phys. Rev. B 30, 5835 (1984).

[40]J. Ihm and J. D. Joannopoulos, Phys. Rev. B 24, 4191 (1983).

[41]P. F. Price, E. N. Maslen, and S. L. Mair, Acta. Crystallogr. A 34, 183 (1978).

[42]B. W. Batterman and D. R. Chipman, Phys. Rev. 127, 690 (1962).

[43]O. H. Nielsen, F. K. Larsen, S. Damgaard, J. W. Petersen, and G. Weyer, Z. Phys. B 52, 99 (1983).

[44]P. M. Raccah, R. N. Euwema, D. J. Stukel, and T. C. Collins, Phys. Rev. B 1, 756 (1970).

[45]A. Zunger, Phys. Rev. B 21, 4785 (1980).

[46]C. S. Wang and B. M. Klein, in Electron Distributions and the Chemical Bond, edited by P. Coppens and M. B. Hall (Plenum, New York, 1982), p. 133.

[47]J. F. Nye, Physical Properties of Crystals (Oxford University Press, Oxford, 1957).

[48]L. Kleinman, Phys. Rev. 128, 2614 (1962); C. S. G. Cousins, J. Phys. C 11, 4867 (1978).

[49]R. M. Martin, Phys. Rev. B 5, 1607 (1972).

[50]H. d'Amour, W. Denner, H. Schulz, and M. Cardona, J. Appl. Crystallogr. 15, 148 (1982).

[51]C. S. G. Cousins, L. Gerward, J. Staun Olsen, B. Selsmark, and B. J. Sheldon, J. Appl. Crystallogr. 15, 154 (1982).

[52]R. Resta and A. Baldereschi, in Ab Initio Calculation of Phonon Spectra, edited by J. T. Devreese, V. E. Van Doren, and P. E. Van Camp (Plenum, New York, 1983).

[53]L. D. Laude, F. H. Pollak, and M. Cardona, Phys. Rev. B 3,

2623 (1971).

[54]L. J. Sham and M. Schlüter, Phys. Rev. Lett. **51**, 1888 (1983).

[55]M. Cardona, in *Light Scattering in Solids II*, edited by M. Cardona and G. Güntherodt, Vol. 51 of *Topics in Applied Physics* (Springer, Berlin, 1982).

[56]N. E. Christensen, Solid State Commun. **50**, 177 (1984).

[57]M. Chandrasekhar, J. B. Renucci, and M. Cardona, Phys. Rev. B **17**, 1623 (1978).

[58]R. N. Thurston and K. Brugger, Phys. Rev. **133**, A1604 (1964); K. Brugger, *ibid*. **133**, A1611 (1964).

[59]V. Heine and D. Weaire, *Solid State Physics*, edited by H. Ehrenreich, F. Seitz, and D. Turnbull (Academic, New York,

1970), Vol. 24, p. 320.

[60]C. S. G. Cousins, J. Phys. C **15**, 1857 (1982).

[61]W. Weber, Phys. Rev. Lett. **33**, 371 (1974); Phys. Rev. B **15**, 4789 (1977).

[62]B. N. Harmon, W. Weber, and D. R. Hamann, Phys. Rev. B **25**, 1109 (1982).

[63]J. Sánches-Dehesa, C. Tejedor, and J. A. Vergés, Phys. Rev. B **26**, 5960 (1982).

[64]M. Cardona, K. Kunc, and R. M. Martin, Solid State Commun. **44**, 1205 (1982).

[65]P. N. Keating, Phys. Rev. **149**, 674 (1966).